Electrochimica Acta 425 (2022) 140720

Contents lists available at ScienceDirect

Electrochimica Acta

journal homepage: www.journals.elsevier.com/electrochimica-acta

# Diffusion in weakly coordinating solvents

Alexander W. Black, Wenjian Zhang, Gillian Reid, Philip N. Bartlett *

*School of Chemistry, University of Southampton, Southampton SO17 1BJ, United Kingdom*

ARTICLE INFO

*Keywords:*
Weakly coordinating solvents
Diffusion coefficients
Ion pairing
Microelectrodes

ABSTRACT

Weakly coordinating solvents are of interest for the electrodeposition of p-block semiconductors for application in electronic devices. p-block complexes typically have weakly coordinated ligands that are easily displaced, making them incompatible with strongly Lewis basic solvents. In this work we use electrochemical measurements at microelectrodes to study diffusion in weakly coordinating solvents. Diffusion coefficients of the metallocenes decamethylferrocene, decamethylferrocenium hexafluorophosphate, cobaltocenium hexafluorophosphate, and the electrodeposition precursors tetrachloroantimonate(III) and tetrachlorobismuthate(III) were measured. The values are analyzed using the modified Stokes-Einstein equation and compared with the theoretical upper, $D_{max}$, and lower, $D_{min}$, bounds of the diffusion coefficients. This approach allows the interpretation of $D$ values, whilst avoiding dealing with some of the uncertainties associated with molecular size in the Stokes-Einstein equation. The neutral decamethylferrocene was found to obey the Stokes-Einstein equation whereas the charged metallocene species had values which were less than the theoretical minimum, which was attributed to a larger than expected particle size caused by ion pairing. The importance of considering the modifications of the Stokes-Einstein equation is also highlighted.

## 1. Introduction

Weakly coordinating solvents are a category of solvent where the molecules are weakly Lewis basic [1]. This means that they are poor ligands and are unlikely to coordinate to a metal cation in a complex. Dichloromethane is one such solvent and its properties as a weakly coordinating solvent have been exploited recently to electrodeposit p-block semiconductors [2–4]. p-block element electrodeposition precursors tend to be labile and hence their ligands are easily displaced, meaning it is important that the solvent will not coordinate to dissolved metal ions. Additional weakly coordinating solvents have also been identified, in order to further the understanding of the nature of electrochemistry in weakly coordinating solvents and to identify alternative solvents to the volatile DCM [1]. The solvents were: α,α,α-trifluorotoluene (TFT), o-dichlorobenzene (oDCB), p-fluorotoluene (pFT), chlorobenzene (CB) and 1,2-dichloroethane (DCE) and these were electrochemically characterised in a recent study.

The diffusion coefficient, $D$, is a constant of proportionality between the flux and the concentration gradient of a diffusing species, and represents the rate of translational movement of a particle. It has a particular importance in electrochemistry since the current response depends on the flux of the electroactive species to the electrode surface. Quantitative descriptions of the current at an electrode require knowledge of the diffusion coefficient and its experimental calculation represents an essential component of the characterisation of a redox couple.

In the present work, the diffusion of neutral and charged species is investigated in the six weakly coordinating solvents: DCM, TFT, oDCB, pFT, CB and DCE in order to improve the understanding of diffusion in this category of solvent. Diffusion coefficients are reported for the neutral decamethylferrocene (DMFc), the cationic decamethylferrocenium hexafluorophosphate ($DMFcPF_6$) and cobaltocenium hexafluorophosphate ($CcPF_6$), and the electrodeposition salts $[N^nBu_4][SbCl_4]$ and $[N^nBu_4][BiCl_4]$. $[SbCl_4]^-$ and $[BiCl_4]^-$ are precursors for the electrodeposition of Sb and Bi that have been used in the electrodeposition of various materials from DCM [3,5,6]. Additionally, oDCB and DCE were recently identified as promising weakly coordinating solvents for semiconductor electrodeposition [1]. Diffusion to the electrode surface is an important factor in the electrodeposition process and it is therefore interesting to study this in greater detail in DCM, oDCB and DCE. Another significant motivation for this work was the desire to be able to predict the diffusion coefficients for new electrodeposition precursors from structural data. The results are examined in the context of the Stokes-Einstein equation, and they are used to understand the nature of diffusion in these solvents. The importance of

* Corresponding author.
*E-mail address:* P.N.Bartlett@soton.ac.uk (P.N. Bartlett).

https://doi.org/10.1016/j.electacta.2022.140720
Received 6 May 2022; Received in revised form 25 May 2022; Accepted 13 June 2022
Available online 16 June 2022

considering the modifications of the Stokes-Einstein equation when interpreting diffusion coefficients is also discussed.

### 1.1. The Stokes-Einstein equation

An accessible approach to the interpretation of diffusion coefficients is with classical hydrodynamic theory and the Stokes-Einstein equation [7]

$$D = \frac{k_B T}{f_{tot}} \quad (1)$$

where $k_B$ is Boltzmann's constant, $T$ is the absolute temperature and $f_{tot}$ is the total friction factor. The term $k_B T$ represents the thermal energy driving force for particle motion, and $f_{tot}$ the friction that impedes it. $f_{tot}$ is then given by

$$f_{tot} = 6\pi\eta r_S \quad (2)$$

where η is the solvent viscosity and $r_S$ is the Stokes radius, the radius of the diffusing species.

However, the Stokes-Einstein equation in its form above carries with it several assumptions that are not always fully appreciated. Firstly, the equation assumes infinite dilution *i.e.* that there are no interactions between diffusing particles. It is also assumed that the solvent is a continuum described only by its viscosity, and finally that the diffusing species is a hard sphere. The Stokes-Einstein equation has proven remarkably effective for large particles, *e.g.* colloids or proteins, but as the size of the particle decreases, theory and experiment begin to diverge, and for molecules of a similar size to the solvent, such as those encountered in electrochemistry, the equation performs poorly [8].

This has resulted in the development of corrections to the Stokes-Einstein equation to improve its description of small molecules. Infinite dilution can be approximated by using low concentrations of analyte. The constant 6 in Eq. (2) can be replaced by the variable $\beta$, which describes the nature of the movement of the diffusing particle past solvent molecules and is proportional to the ratio of the radii of the solvent and solute molecules. $\beta$ decreases as the ratio increases, to the lower limit of 4, such that $4 \leq \beta \leq 6$, therefore accounting for non-continuum effects. The motion when $\beta = 4$ is commonly referred to as 'slipping', and when $\beta = 6$ as 'sticking'. Expressions for its exact estimation have been provided by Gierer and Wirtz, and Chen and Chen [9]. Corrections for a diffusing species that is non-spherical can also be found. Perrin provided corrections for ellipsoids of revolution, a more common shape in electrochemistry [10]. $f_{tot}$ then becomes

$$f_{tot} = f_{HS} f_P \quad (3)$$

where $f_{HS}$ is the hard-sphere friction factor, equal to $c\pi\eta r_S$, and $f_P$ is the Perrin correction.

There is also the question of how best to estimate the radius of the particle in solution. There are several radii that can be found in the literature for polyatomic molecules, obtained using different methods and it is not clear which most accurately describes their size in solution [11]. Furthermore, molecules can be uneven and irregular, creating a non-uniform surface and variations in their radius across it. From experiments, Macchioni et al. concluded that the upper and lower limits of $r_S$ are the crystallographic radius, $r_{crs}$, and the van der Waals radius, $r_{vdW}$, respectively [12]. $r_{crs}$ is obtained from X-ray crystal structure measurements, the calculated unit cell volume can be converted into a radius by assuming sphericity [12]. $r_{crs}$ describes the space occupied by the molecule plus void spaces between molecules due to repulsive forces. $r_{vdW}$ is taken from the van der Waals volume, $V_{vdW}$, which is the sum of the spheres occupied by the constituent atoms, after accounting for bonding. $V_{vdW}$ is obtained from computational calculations, or from correlation with other radii [11].

Another common approach to correlating diffusion coefficients is with the Wilke-Chang equation [13]. This is an empirical modification of the Stokes-Einstein equation, obtained from data for a range of (typically organic) solutes and solvents. Here, $D$ is proportional to $(M_r)^{1/2}/\eta V^{0.6}$, where $M_r$ is the relative molecular mass of the diffusing species, and $V$ is its molal volume. The Wilke-Chang equation is often used in electrochemistry, as an alternative to the Stokes-Einstein equation, to predict and analyze experimental diffusion coefficients, as in Refs. [14–16] for example. The Wilke-Chang equation also requires a 'solvent association parameter', which describes the strength of interactions between solvent molecules *e.g.* hydrogen bonding [13,17]. This property must be determined experimentally, and so makes it difficult to apply the equation to solvents for which little data is available. The molecular mass approach has also been extended to allow diffusion coefficients to be directly correlated with $M_r$, using a method developed by Valencia and Gonzalez which was based upon electrochemical measurements of various organic molecules in acetonitrile, dimethylsulfoxide and N,N-dimethylformamide [18,19].

Approaches based on correlation with $M_r$ assume that, for a given solvent, the density remains constant across the measured dataset. This is likely to be true for organic molecules, as evidenced by the success of the Wilke-Chang equation for such compounds, however in this work where organometallic complexes and p-block halometallate complexes are studied, it cannot be known with any certainty that this is the case. Furthermore, Zaccaria et al. measured the diffusion of multiple organometallic complexes with approximately the same size and shape, but differing metal centres and so different molecular masses [20]. It was found that the size of the molecule, rather than weight, was the determining factor in their diffusion properties. As such, correlations based on molecular mass are not considered appropriate for the compounds under investigation here, and the more general Stokes-Einstein equation is preferred.

## 2. Experimental

### 2.1. Chemicals

Dichloromethane, $CH_2Cl_2$ (95%, Sigma-Aldrich), α, α, α-trifluorotoluene, $C_7H_5F_3$ (>99%, Sigma-Aldrich), *o*-dichlorobenzene, $C_6H_4Cl_2$ (>99%, Sigma-Aldrich), *p*-fluorotoluene, $C_7H_7F$ (97%, Sigma-Aldrich), chlorobenzene, $C_6H_5Cl$ (>99%, Sigma-Aldrich) and 1,2-dichloroethane, $H_2ClCCH_2Cl$ (>99%, Sigma-Aldrich) were dried and degassed by refluxing with $CaH_2$ under a dinitrogen atmosphere followed by distillation, and were stored in an inert atmosphere of $N_2$. The water content in the solvents was measured with Karl–Fischer titration (KF 899 Coulometer, Metrohm, UK). There was less than 35 ppm of water in all solvents. Tetrabutylammonium chloride, $[N^nBu_4]Cl$ (Sigma-Aldrich, >99%) and tetrabutylammonium tetrafluoroborate, $[N^nBu_4][BF_4]$ (Sigma-Aldrich, >99%) were dried by heating at 100 °C under vacuum for several hours. Decamethylferrocene, $[\{C_5(CH_3)_5\}_2Fe]$ (Sigma-Aldrich, 97%) and cobaltocenium hexafluorophosphate, $[(C_5H_5)_2Co][PF_6]$ (Sigma-Aldrich, 98%) were purified by sublimation. Decamethylferrocenium hexafluorophosphate, $[\{C_5(CH_3)_5\}_2Fe][PF_6]$, was synthesised according to a procedure by Duggan and Hendrickson [21]. Tetrabutylammonium tetrachloroantimonate(III), $[N^nBu_4][SbCl_4]$ and tetrabutylammonium tetrachlorobismuthate(III), $[N^nBu_4][BiCl_4]$ were prepared using methods previously described in the literature [22]. All solvents and reagents were stored in a dry, $N_2$ purged glovebox.

### 2.2. Electrodes

Working electrodes used were inlaid Pt microdiscs of radii 5, 12.5 and 25 μm, sealed in glass. The working electrodes were polished sequentially with 5, 1 and 0.3 μm alumina pastes on a microcloth polishing pad (Buehler, USA). Microelectrodes were calibrated using SEM (Philips XL30 ESEM). A Pt grid was used as a counter electrode, the

reference electrode was Ag/AgCl immersed in a storage solution of 100 mM $[N^nBu_4]Cl$ for dichloromethane, *o*-dichlorobenzene and 1,2-dichloroethane, separated from the electrolyte by a porous glass frit, and a Pt wire pseudo reference for α, α, α-trifluorotoluene, *p*-fluorotoluene and chlorobenzene.

### 2.3. Electrochemical measurements

All glassware was cleaned by soaking in Decon 90 (Decon Laboratories Ltd., UK) for at least 24 h, followed by rinsing with ultrapure water, 0.055 μS $cm^{-1,}$ and then dried in an oven for a further 24 h. All experiments were performed with a standard pear-shaped cell in a glovebox (Belle Technology, UK) under an inert atmosphere of $N_2$ in the presence of <5 ppm $O_2$ and $H_2O$. Measurements were performed with a PGSTAT μIII (Metrohm Autolab, UK) potentiostat. Data was recorded with NOVA 1.11 (Metrohm Autolab, UK). The ambient temperature in the glovebox was monitored using a digital thermometer to an accuracy of ±0.05 °C (Hama, UK).

## 3. Results

Diffusion coefficients of DMFc and $CcPF_6$ have been reported previously in the studied weakly coordinating solvents and were taken from Ref. [1], with their values given in Table 1. Voltammograms of $DMFc^+$, $[SbCl_4]^-$ and $[BiCl_4]^-$ were collected at Pt microelectrodes of radii 5, 12.5 and 25 μm. Representative microelectrode voltammograms for $DMFcPF_6$ can be found in Fig. 1. As can be seen, a limiting current plateau is present for the voltammograms at every size of electrode in every solvent, indicating a mass transport limited redox reaction. Voltammograms for $[SbCl_4]^-$ and $[BiCl_4]^-$ can be found in Fig. S1. Diffusion coefficients were then obtained from the slope of a plot of limiting current *vs.* microelectrode radius for three different sizes of microelectrode, since

$$i_L = 4nFDca \quad (4)$$

where $i_L$ is the limiting current, $n$ is the number of electrons transferred, $F$ is the Faraday, $c$ is concentration of electroactive species and $a$ is the radius of the electrode. $n$ was taken as 1 for $DMFcPF_6$, and 3 for $[SbCl_4]^-$ and $[BiCl_4]^-$. Representative plots of $i_L$ *vs.* $a$ are shown in Fig. 2 for $DMFcPF_6$, clearly the plots are linear with intercepts close to the origin demonstrating the validity of Eq. (4). Plots for $[SbCl_4]^-$ and $[BiCl_4]^-$ are then given in Fig. S2. The microelectrode radii were calibrated using SEM to give the effective geometric radius of the microelectrode, and the effective concentration in solution was obtained from a potential step at a microelectrode and fitting to the Shoup-Szabo equation [23]. The average of the concentration at each microelectrode was then used as $c$. Calculating diffusion coefficients in this way improves the accuracy of the resulting value because it can smooth out any individual errors associated with $i_L$, $c$ or $a$. Potential steps were not performed for $[SbCl_4]^-$ and $[BiCl_4]^-$ and so the weighed concentration was used.

Measured diffusion coefficients, along with some relevant physical properties for the solvents can be found in Table 1. $D$ was also calculated from potential step data for $DMFcPF_6$, and corroborates the values in Table 1 (see Table S1). Work has shown previously that CVs and potential steps at a microelectrode are two of the most accurate and precise methods for measuring diffusion coefficients [24]. Microelectrodes are also particularly useful in solvents of relatively low polarity, such as those studied here. The small current response minimises distortions associated with *iR* drop.

The measured diffusion coefficients are in agreement with those reported in the literature, Goldfarb and Corti also reported a value of $1.07 \times 10^{-5}$ $cm^2$ $s^{-1}$ for $DMFcPF_6$ in DCM at 25 °C [25]. Reeves et al. found $D$ for $[N^nBu_4][SbCl_4]$ in DCM at 25 °C to be $9.2 \times 10^{-6}$ $cm^2$ $s^{-1}$. [5].

**Table 1**
Selected physical properties and experimental diffusion coefficients at 25 °C of redox couples in weakly coordinating solvents. Diffusion coefficients obtained from the limiting current at a microelectrode. Each value is the average of three repeats and the error the standard deviation.

| Solvent | $\varepsilon_r$[a] | η / mPa s | $D$ / $10^{-5}$ $cm^2$ $s^{-1}$ | | | | |
|---|---|---|---|---|---|---|---|
| | | | $DMFc$[d] | $DMFc^+$ | $Cc^+$[d] | $[SbCl_4]^-$ | $[BiCl_4]^-$ |
| DCM | 8.9 | 0.41[a] | 1.68(2) | 1.21 (3) | 1.35 (1) | 0.83(7) | 0.73(3) |
| TFT | 9.2 | 0.47[b] | 1.18(3) | 0.76 (1) | 0.38 (2) | – | – |
| oDCB | 9.9 | 1.32[a] | 0.52(1) | 0.35 (1) | 0.24 (1) | 0.18(1) | 0.19(1) |
| pFT | 5.9 | 0.62[c] | 1.10 (11) | 0.47 (2) | 0.31 (3) | – | – |
| CB | 5.6 | 0.76[a] | 0.87(3) | 0.46 (1) | 0.32 (2) | – | – |
| DCE | 10.4 | 0.78[a] | 0.88(3) | 0.53 (1) | 0.61 (3) | 0.43(1) | 0.37(2) |

[a] Ref. [26].
[b] Ref. [27].
[c] Ref. [28].
[d] Ref. [1].

## 4. Discussion

The first step towards analysing diffusion coefficients in multiple solvents with the Stokes Einstein equation is to make a plot of $D$ *vs.* $\eta^{-1}$. If the plot is linear with an intercept close to the origin, the equation can be considered valid and insight can be gained into the size of the diffusing species from the slope of the plot. However, addition of electrolyte to a solvent increases the viscosity of the solution relative to the pure solvent and this must be taken into account. The increase in solvent viscosity with electrolyte addition is described by the Jones-Dole equation [29]. This was used to estimate the relative viscosity, $\eta_{rel}$, where data was available, for the electrolyte solutions studied here. Further details and values can be found in Section S4 of the SI. The ratio of electrolyte to solvent viscosity is taken as 1.102 for all solvents and electrolytes.

Calculation of the Perrin correction for non-sphericity, $f_P$, requires knowledge of the dimensions of the molecules. These were obtained from crystal structure data using visualisation software. The resulting values for $f_P$ were 1.002 and 1.004 for DMFc and $Cc^+$, respectively, indicating that the molecules are essentially spherical and the Perrin correction can be ignored. Details of the calculation of $f_P$ are given in SI Section S3. The size of DMFc does not change significantly upon oxidation and so $DMFc^+$ can also be considered spherical. Moments of inertia measurements additionally suggest that $DMFc^+$ is spherical [30]. Reeves et al. used bond lengths and the geometry of the $[SbCl_4]^-$ anion to calculate $f_P$ and concluded that the ion was spherical and that no correction was required [5], and this is also assumed to be true in the present work. Spectroscopic measurements indicate that $[BiCl_4]^-$ has a similar geometry to $[SbCl_4]^-$ and so is not expected to need correcting either [31].

Beginning with the neutral DMFc, a Stokes-Einstein plot of $D_{exp}$ *vs.* $\eta^{-1}$, where $D_{exp}$ is the experimental diffusion coefficient, is shown in Fig. 3 in black, using the corrected viscosity values. As can be seen, the plot is linear with an intercept close to zero and so it can be concluded that DMFc obeys the Stokes-Einstein equation in these weakly coordinating solvents.

As described above: $4 \leq \beta \leq 6$ and $r_{vdW} \leq r_S \leq r_{crs}$. Therefore, the experimental diffusion coefficient can be expected to lie within the upper bound, $D_{max}$, when $\beta = 4$, $r = r_{vdW}$ and the lower bound, $D_{min}$ when $\beta = 6$ and $r = r_{crs}$. $D_{min}$ and $D_{max}$ were calculated for DMFc in the studied solvents and the results are also plotted on Fig. 3. Further details of the methods to obtain the molecular radii and the resulting diffusion coefficients can be found in Sections S5 and S6 of the SI, respectively. As

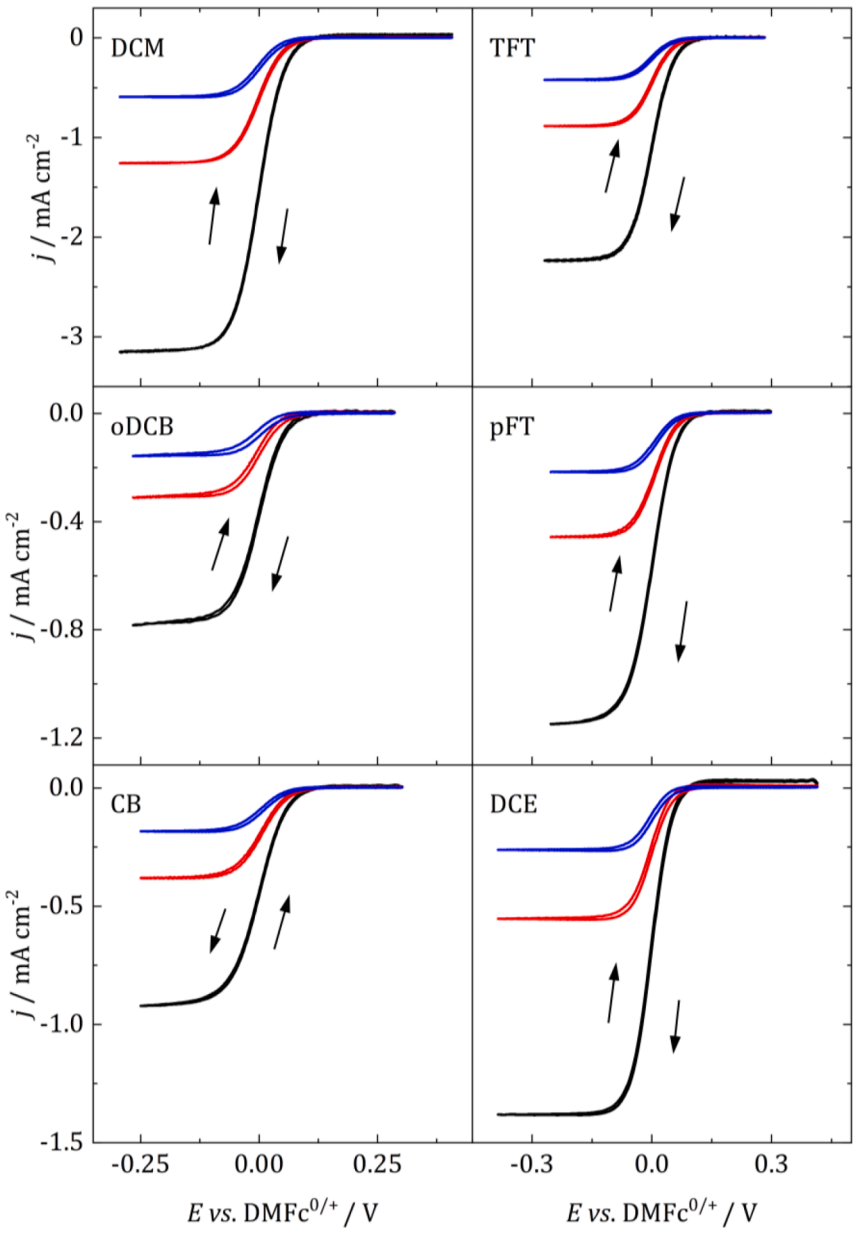


**Fig. 1.** Representative microelectrode voltammograms for 1 mM $DMFcPF_6$ with 100 mM $[N^nBu_4]Cl$ at a Pt WE. Potential scanned in the direction of the arrows at a sweep rate of 5 mV $s^{-1}$. CE: Pt grid, DCM, oDCB, DCE: Ag/AgCl RE, TFT, pFT, CB: Pt QRE. Black: $r = 5$ μm, red: $r = 12.5$ μm, blue: $r = 25$ μm.

can be seen, $D_{exp}$(DMFc) matches closely with $D_{max}$, suggesting that for DMFc, $\beta \approx 4$ and $r_S \approx r_{vdW}$. This can readily be rationalised since $\beta$ approaches four as the radius of the solvent molecule and the diffusing particle become similar in size. Taking the radius of DCM as 2.5 Å for example [5], this is similar to the vDW radius for DMFc of 4.2 Å (see SI). Additionally, $r_S$ is typically found to be close to $r_{vdW}$ for small, compact molecules [12].

This approach to analysing the diffusion coefficient makes no assumptions about β or $r$ and so avoids any of the uncertainties associated with these values, whilst also giving insight into the size of the particle in solution and its interaction with the solvent. It also emphasises the importance of considering modifications to the Stokes-Einstein equation when analysing diffusion coefficients. Often, $r_S$ is calculated from the slope of the Stokes-Einstein plot, if $\beta$ was taken as six then this would lead to a misleading value of $r_S$ for DMFc.

To prove that the approach outlined above is a useful method of analysis rather than simply fortuitous agreement for the solvents studied here, diffusion coefficients of DMFc in different solvents were compiled from the literature and plotted along with their $D_{min}$ and $D_{max}$, in Fig. 4. The values are tabulated in Table S7. As can be seen, excepting a few outliers, all the reported values for the diffusion coefficient of DMFc lie within $D_{min}$ and $D_{max}$. The three data points with the largest discrepancy, one for THF and two from DCM, are all from the same source, Ref. [32], suggesting there may have been a systematic difference in the measurement of $D$.

It is noteworthy that where there are multiple data points for the same solvent that, even for DMFc a relatively simple system, a large variation in $D$ is observed in the literature values determined electrochemically. This emphasises the importance of careful attention to details including temperature control, accurate measurement of electrode dimensions and solute concentration. It is also worth pointing out that the use of microelectrodes, as opposed to macrodisc cyclic voltammetry, avoids problems of iR drop and gives currents that are proportional to $D$ rather than to $D^{1/2}$.

It is also interesting to investigate the diffusion of charged species to study any changes in behavior as a result of ion formation. The cationic

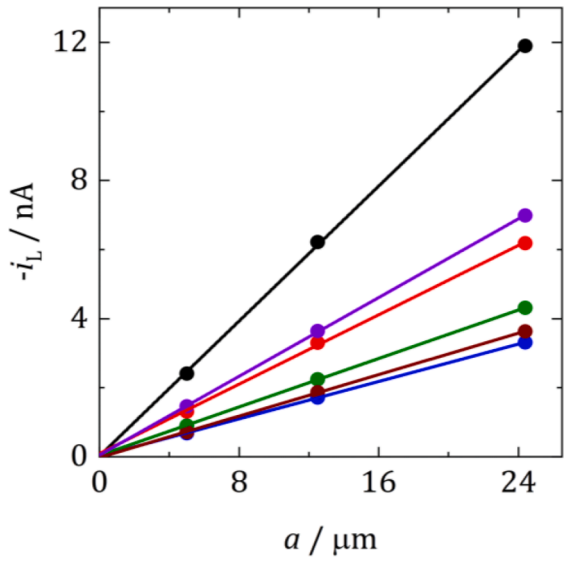


**Fig. 2.** Limiting currents for 1 mM $DMFcPF_6$ at Pt microelectrodes of radii $r$ = 5 μm, 12.5 μm and 25 μm. Black: DCM, red: TFT, blue: oDCB, green: pFT, brown: CB, purple: DCE.

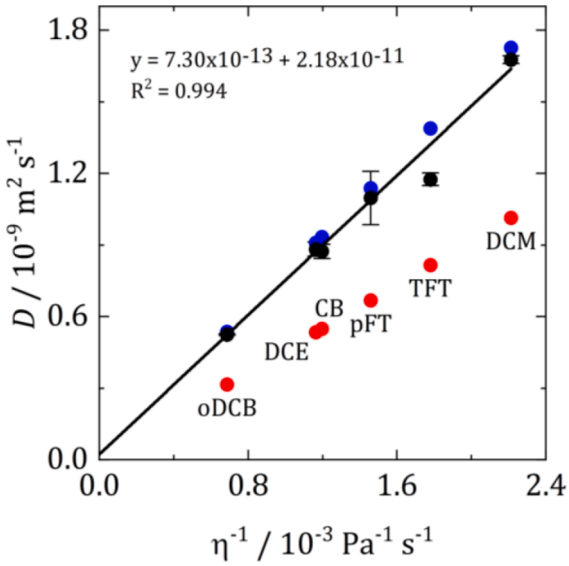


**Fig. 3.** Stokes-Einstein plot of experimental diffusion coefficients for DMFc in weakly coordinating solvents at 25 °C along with simulated $D_{min}$ and $D_{max}$. Black: $D_{exp}$, red: $D_{min}$, blue: $D_{max}$.

metallocenes, decamethylferrocenium hexafluorophosphate ($DMFcPF_6$) and cobaltocenium hexafluorophosphate ($CcPF_6$) were initially used for this purpose. Stokes-Einstein plots for both, along with $D_{min}$ and $D_{max}$ are shown in Fig. 5. For $DMFc^+$ the same $D_{min}$ and $D_{max}$ as DMFc was used, and details for $Cc^+$ can be found in the SI. Clearly, the situation is different for charged species, and linear Stokes-Einstein behavior is no longer observed for $DMFc^+$ nor $Cc^+$. The measured diffusion coefficients for both redox couples are now lower than their minimum theoretical value of $D_{max}$. A dramatic increase in viscosity as a result of the addition of the redox couples at these concentrations (100 mM) is not plausible. Therefore, it appears that the radius of the diffusing species, $r_S$, is larger than that predicted by theory.

There are no major changes to the structure of DMFc and Cc upon oxidation, except for the fact that they are now charged. Therefore, the most plausible explanation for $r_S$ to be greater than expected is the presence of ion pairing. If $DMFc^+$ and $Cc^+$ were associating with the $Cl^-$

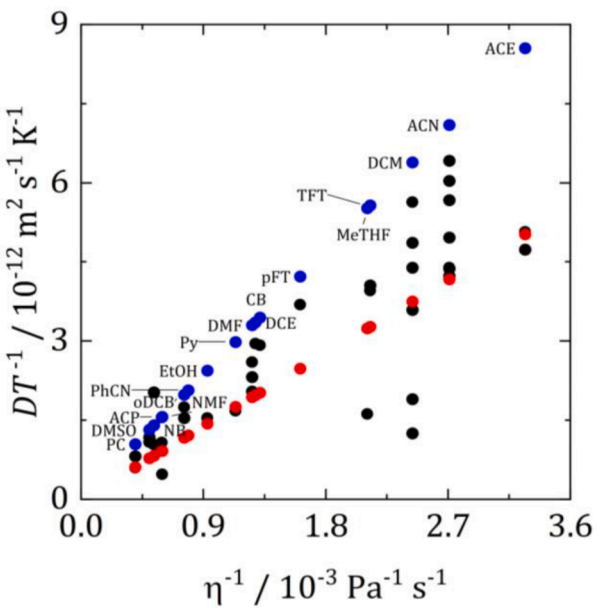


**Fig. 4.** Stokes-Einstein plot of experimental DMFc diffusion coefficients normalised with respect to temperature compiled from the literature together with calculated $D_{min}$ and $D_{max}$ values. See text for details of $D_{min}$ and $D_{max}$, and SI for compilation. Black: $D_{exp}$, red: $D_{min}$, blue: $D_{max}$.

or $[BF_4]^-$ ion then this would form a larger diffusing particle. This is reasonable when considering the low polarity of the solvents, where the degree of ion pairing is expected to be high. $DMFc^+$ was found to have a lower diffusion coefficient than DMFc in DCM by Goldfarb and Corti, in agreement with the results presented here [25]. Conductivity measurements in the literature also indicate the presence of ion pairing in these solvents. The association constant, $K_A$, describes the position of the equilibrium between free ions and ion pairs. The greater $K_A$ is above 1, the more that ion pairs are favoured in the electrolyte. Table S9 shows a compilation of relevant association constants from the literature. $K_A$ is significantly greater than 1 for all the electrolytes where data is available, therefore clearly showing that a significant fraction of ions can be expected to be paired in the solvents studied here.

The presence of triple ions is also possible. Fuoss [33] provided a rule of thumb for the maximum concentration, $c_{max}$, at which only ion pairs are expected for a symmetrical electrolyte, and above which triple ions could be expected to be observed:

$$c_{max} = 1.2x10^{-14}(\varepsilon_r T)^3 \quad (5)$$

taking the largest dielectric constant of 10.4 for DCE at 298 K gives $c_{max}$ of 0.4 mM. This is of a similar order to the concentrations used here, meaning the presence of triple ions in these solvents is probable. The measured diffusion coefficients can then be considered as a weighted average of the diffusion coefficient of all forms of the electroactive species in solution.

The presence of any ion pairs or triplets can be explored by calculating $r_S$ from the diffusion coefficients of $DMFc^+$ and $Cc^+$. This was achieved by taking $\beta$ as 4 (a reasonable assumption considering the data for DMFc above) and results are given in Table 2. These values represent an upper bound for $r_S$, since $\beta$ would increase above 4 if it was estimated using the radii of the diffusing particle and the solvent. Using 0.48 nm as a value of $r(DMFc^+)$ and $r(Cc^+)$ as 0.38 nm (see SI), and also $r(Cl^-)$ as 0.18 nm and $r([BF_4]^-)$ as 0.23 nm (Ref. [34]), the approximate size of an ion pair can be estimated (Table 2). The experimental $r_S$ can then be compared with the radii of the bare ions and also the ion pair. For $DMFc^+$ and $Cc^+$ in DCM, $r_S$ is in between the free ion and the estimate for the ion pair, suggesting that here the ions exist as a mixture of both forms. For $DMFc^+$ in oDCB, and also both species in DCE, $r_S$ is similar to

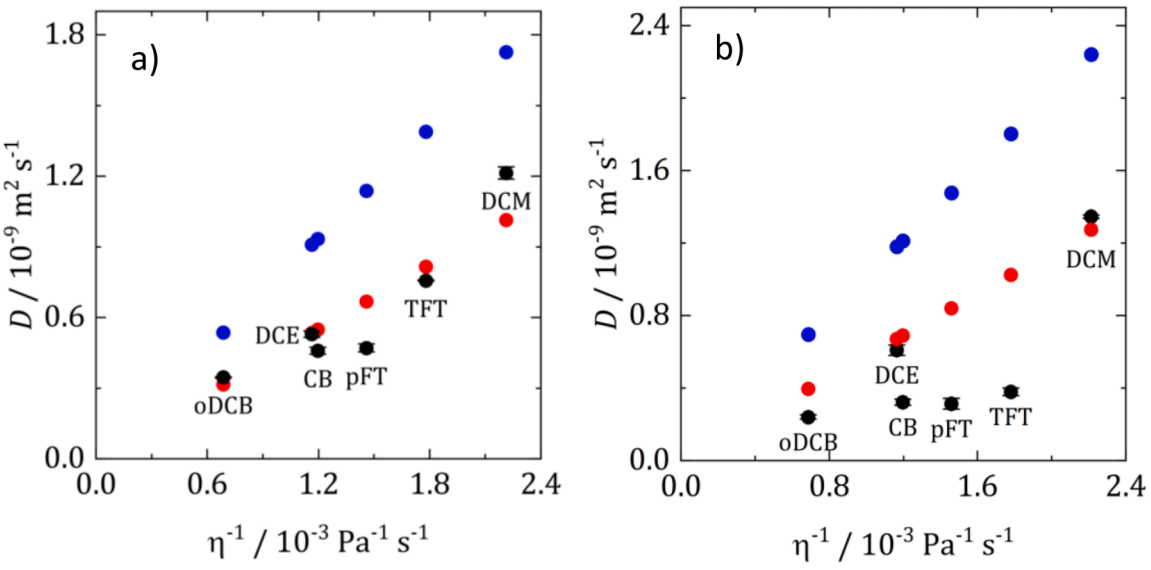


**Fig. 5.** Experimental Stokes-Einstein plots for (a) $DMFcPF_6$ and (b) $CcPF_6$ at 25 °C along with simulated $D_{max}$ and $D_{min}$ for $Cc^+$ and DMFc. Black: $D_{exp}$, red: $D_{min}$, blue: $D_{max}$.

**Table 2**
The Stokes radii, $r_S$, of $DMFc^+$ and $Cc^+$, determined from diffusion coefficients, and an estimate of the size of an ion pair for each species.

| Solvent | $r_S(DMFc^+)$ / nm | $r_S(Cc^+)$ / nm | Estimated radius | |
|---|---|---|---|---|
| DCM | 0.60 | 0.54 | $r(DMFc^+)$ 0.48 nm | $r(Cc^+)$ 0.38 nm |
| oDCB | 0.65 | 0.94 | $r(DMFc^+ + Cl^-)$ | $r(Cc^+ + Cl^-)$ |
| DCE | 0.72 | 0.63 | 0.66 nm | 0.56 nm |
| TFT | 0.77 | 1.54 | $r(DMFc^+)$ 0.48 nm | $r(Cc^+)$ 0.38 nm |
| pFT | 1.02 | 1.52 | $r(DMFc^+ + [BF_4]^-)$ | $r(Cc^+ + [BF_4]^-)$ |
| CB | 0.85 | 1.22 | 0.71 nm | 0.61 nm |

the estimate for the size of the ion pair so these are probably mostly present in the form of ion pairs. $r_S$ is then greater than the ion pair radius in the remaining electrolytes, which could point to the presence of triple ions. It is noticeable that $r_S$ for $Cc^+$ is larger than that for $DMFc^+$ in oDCB, CB, TFT and pFT consistent with greater ion association for the smaller, and therefore higher charge density, $Cc^+$ ion. It must also be noted that interpretation of Stokes radii in this way must be done with caution and care must be taken not to over interpret the data [35].

Fig. 6 shows Stokes-Einstein plots for $[SbCl_4]^-$ and $[BiCl_4]^-$ in the three solvents. Also shown are their simulated $D_{max}$ and $D_{min}$ values. $r_{vdW}$ and $r_{crs}$ were not available for either metal complex so the McGowan radius, $r_{McG}$, from the McGowan volume was used instead [26]. This is an intrinsic volume based upon the additive volumes of the constituent atoms and is intermediate between $r_{vdW}$ and $r_{crs}$ [26]. The simulated $D_{max}$ and $D_{min}$ are given in Table S6.

The plots in Fig. 6 appear linear, however the intercept is much less than zero, suggesting that the precursors are not behaving according to the Stokes-Einstein equation. Furthermore, as was the case for the cationic species above, $D_{exp}$ of these anionic complexes is lower than the simulated $D_{min}$, indicating that $r_S$ is greater than expected. This can be attributed to the presence of ion pairing once again, where now the anions are paired with the $[N^nBu_4]^+$ cation. The formation of chloride

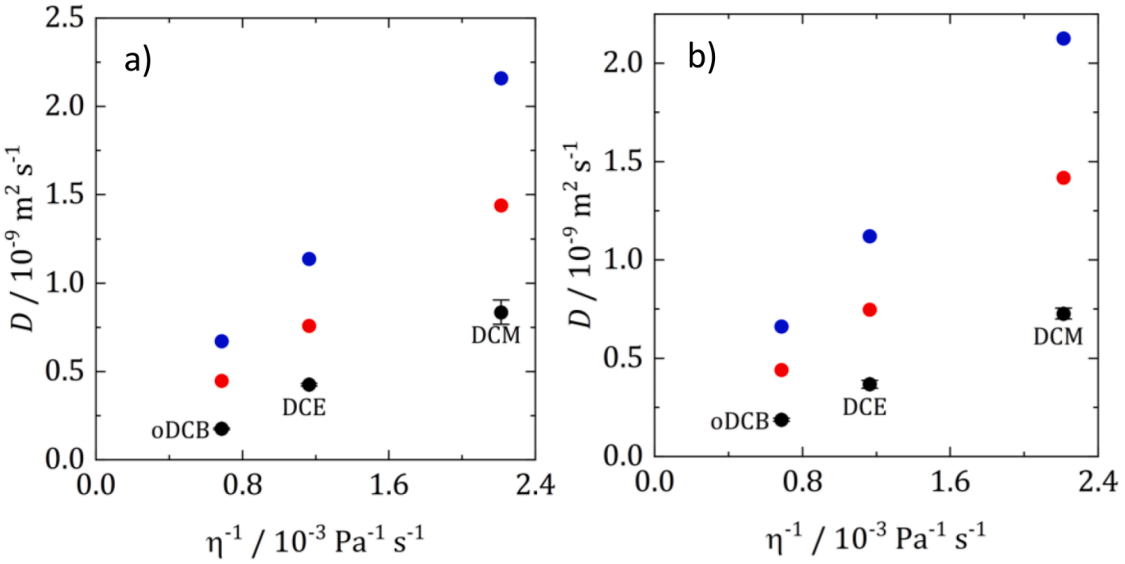


**Fig. 6.** Experimental Stokes-Einstein plots for (a) $[N^nBu_4][SbCl_4]$ and (b) $[N^nBu_4][BiCl_4]$ in DCM, oDCB and DCE at 25 °C along with simulated $D_{max}$ and $D_{min}$. Black: $D_{exp}$, red: $D_{min}$ and blue: $D_{max}$.

bridged dimers and higher oligomers of the metal complexes in solution is also possible [36], and has been observed previously in crystal structures of the chlorometallate salts [37,38]. These would be in equilibrium with the monomer and could also cause a larger than predicted diffusing species, similar to ion pairing. Although the two effects are likely to be indistinguishable from each other with diffusion coefficient measurements.

## 5. Conclusion

This work used electrochemical methods to measure the diffusion coefficients of neutral, cationic and anionic redox couples in weakly coordinating solvents. The resulting values were then analyzed using the Stokes-Einstein equation, and plots of $D$ *vs.* $\eta^{-1}$. For the neutral DMFc, a linear plot was observed, indicating that the Stokes-Einstein equation was obeyed. The theoretical upper and lower bounds, $D_{max}$ and $D_{min}$, respectively, were also calculated and compared to the experimental values. The experimental measurements were similar to $D_{max}$ and it was possible to conclude that $r_S$(DMFc) was close to $r_{vdW}$ in these solvents, and that the particles moved through the solvent with 'slipping' motion. This approach allows analysis of diffusion coefficients, and the comparison of theory with experiment, whilst avoiding the assignment of definite values to the radii of the solvent or particle in solution, which can often be uncertain.

The cationic $DMFc^+$ and $Cc^+$, and the anionic $[SbCl_4]^-$ and $[BiCl_4]^-$ were also studied. In contrast with neutral DMFc, these charged species had diffusion coefficients that were less than their theoretical lower bound. Due to the low polarity of the weakly coordinating solvents, this was attributed to a larger than expected $r_S$ caused by ion pairing with the anions or cations of the supporting electrolyte.

When interpreting diffusion coefficients with the Stokes-Einstein equation, it is clearly essential to consider its modifications in order to properly understand diffusion behavior and draw robust conclusions. Improper consideration of them has the potential to lead to the calculation of erroneous values for $r_S$, which can lead to misinterpretation of the size of the diffusing species in solution. It is also important for the calculation of accurate diffusion coefficients to ensure that the electrode size and solute concentration are properly measured.

Conceptually, radii taken from the partial molar volume, $V_{m,i}$, would appear to be the most accurate measure of the size of a species, since this is its volume contribution measured at exactly the same electrolyte composition as that used to measure the diffusion coefficient [39]. Knowledge of this would negate the approach using $r_{vdW}$ and $r_{crs}$ and would improve the accuracy of diffusion coefficient predictions. However, $V_{m,i}$ is an experimentally derived parameter that is difficult to measure and also to predict. Furthermore, ideally an exact value for $\beta$ would be calculated, however finding a consistent method of measuring the sizes of organic molecules, metal complexes and salts is not a simple task. Meaning it is difficult to obtain uniform values of the radius of the solvent as well as the electroactive species. Some of the solvent molecules are also aromatic, and so disc shaped rather than spherical. Their size would most accurately be described by two axes, and it is currently not possible to incorporate this into the available methods of estimating $\beta$.

## CRediT authorship contribution statement

**Alexander W. Black:** Conceptualization, Methodology, Validation, Formal analysis, Investigation, Data curation, Writing – original draft, Visualization. **Wenjian Zhang:** Resources. **Gillian Reid:** Methodology, Conceptualization, Resources, Writing – review & editing, Supervision. **Philip N. Bartlett:** Conceptualization, Methodology, Validation, Formal analysis, Writing – review & editing, Supervision, Funding acquisition, Project administration.

## Declaration of Competing Interest

None.

## Acknowledgments

This work was supported by the EPSRC through the Advanced Devices by Electroplating program grant (ADEPT; EP/N035437/1). All data supporting this study are openly available from the University of Southampton repository at https://doi.org/10.5258/SOTON/D2211.

## Supplementary materials

Supplementary material associated with this article can be found, in the online version, at doi:10.1016/j.electacta.2022.140720.

## References

[1] A.W. Black, P.N. Bartlett, Selection and characterisation of weakly coordinating solvents for semiconductor electrodeposition, Phys. Chem. Chem. Phys. 24 (2022) 8093–8103, https://doi.org/10.1039/D2CP00696K.
[2] A.H. Jaafar, L. Meng, Y.J. Noori, W. Zhang, Y. Han, R. Beanland, D.C. Smith, G. Reid, K. De Groot, R. Huang, P.N. Bartlett, Electrodeposition of GeSbTe-based resistive switching memory in crossbar arrays, J. Phys. Chem. C 125 (2021) 26247–26255, https://doi.org/10.1021/acs.jpcc.1c08549.
[3] Y.J. Noori, L. Meng, A.H. Jaafar, W. Zhang, G.P. Kissling, Y. Han, N. Abdelazim, M. Alibouri, K. Leblanc, N. Zhelev, R. Huang, R. Beanland, D.C. Smith, G. Reid, K. De Groot, P.N. Bartlett, Phase-change memory by GeSbTe electrodeposition in crossbar arrays, ACS Appl. Electron. Mater. 3 (2021) 3610–3618, https://doi.org/10.1021/acsaelm.1c00491.
[4] N.M. Abdelazim, Y.J. Noori, S. Thomas, V.K. Greenacre, Y. Han, D.E. Smith, G. Piana, N. Zhelev, A.L. Hector, R. Beanland, G. Reid, P.N. Bartlett, C.H. de Groot, Lateral growth of MoS2 2D material semiconductors over an insulator via electrodeposition, Adv. Electron. Mater. 7 (2021), 2100419, https://doi.org/10.1002/aelm.202100419.
[5] S.J. Reeves, Y.J. Noori, W. Zhang, G. Reid, P.N. Bartlett, Chloroantimonate electrochemistry in dichloromethane, Electrochim. Acta 354 (2020), 136692, https://doi.org/10.1016/j.electacta.2020.136692.
[6] K. Cicvarić, L. Meng, D.W. Newbrook, R. Huang, S. Ye, W. Zhang, A.L. Hector, G. Reid, P.N. Bartlett, C.H.K. De Groot, Thermoelectric properties of bismuth telluride thin films electrodeposited from a nonaqueous solution, ACS Omega 5 (2020) 14679–14688, https://doi.org/10.1021/acsomega.0c01284.
[7] H.J.V. Tyrell, K.R. Harris, Diffusion in Liquids, Butterworths, London, 1984.
[8] D. Fennell Evans, T. Tominaga, C. Chan, Diffusion of symmetrical and spherical solutes in protic, aprotic, and hydrocarbon solvents, J. Solut. Chem. 8 (1979) 461–478, https://doi.org/10.1007/BF00716005.
[9] R. Evans, G. Dal Poggetto, M. Nilsson, G.A. Morris, Improving the interpretation of small molecule diffusion coefficients, Anal. Chem. 90 (2018) 3987–3994, https://doi.org/10.1021/acs.analchem.7b05032.
[10] P.F. Perrin, Mouvement brownien d'un ellipsoide - I. Dispersion diélectrique pour des molécules ellipsoidale, J. Phys. Radium 5 (1934) 497–511, https://doi.org/10.1051/jphysrad:01934005010049700.
[11] Y. Marcus, The sizes of molecules - revisited, J. Phys. Org. Chem. 16 (2003) 398–408, https://doi.org/10.1002/poc.651.
[12] A. Macchioni, G. Ciancaleoni, C. Zuccaccia, D. Zuccaccia, Determining accurate molecular sizes in solution through NMR diffusion spectroscopy, Chem. Soc. Rev. 37 (2008) 479–489, https://doi.org/10.1039/b615067p.
[13] C.R. Wilke, P. Chang, Correlation of diffusion coefficients in dilute solutions, AIChE J. 1 (1955) 264–270, https://doi.org/10.1002/aic.690010222.
[14] S.R. Jacob, Q. Hong, B.A. Coles, R.G. Compton, Variable-temperature microelectrode voltammetry: application to diffusion coefficients and electrode reaction mechanisms, J. Phys. Chem. B 103 (1999) 2963–2969, https://doi.org/10.1021/jp990024w.
[15] F.J. Del Campo, E. Maisonhaute, R.G. Compton, F. Marken, A. Aldaz, Low-temperature sonoelectrochemical processes - part 3. Electrodimerisation of 2-nitrobenzylchloride in liquid ammonia, J. Electroanal. Chem. 506 (2001) 170–177, https://doi.org/10.1016/S0022-0728(01)00501-0.
[16] N.V. Rees, J.D. Wadhawan, O.V. Klymenko, B.A. Coles, R.G. Compton, An electrochemical study of the oxidation of 1,3,5-Tris[4-[(3-*methylphenyl*) *phenylamino*]phenyl]benzene, J. Electroanal. Chem. 563 (2004) 191–202, https://doi.org/10.1016/j.jelechem.2003.08.034.
[17] B.A. Parsons, D.K. Pinkerton, R.E. Synovec, Implications of phase ratio for maximizing peak capacity in comprehensive two-dimensional gas chromatography time-of-flight mass spectrometry, J. Chromatogr. A 1536 (2018) 16–26, https://doi.org/10.1016/j.chroma.2017.07.018.
[18] D.P. Valencia, F.J. González, Understanding the linear correlation between diffusion coefficient and molecular weight. A model to estimate diffusion coefficients in acetonitrile solutions, Electrochem. Commun. 13 (2011) 129–132, https://doi.org/10.1016/j.elecom.2010.11.032.

[19] D.P. Valencia, F.J. González, Estimation of diffusion coefficients by using a linear correlation between the diffusion coefficient and molecular weight, J. Electroanal. Chem. 681 (2012) 121–126, https://doi.org/10.1016/j.jelechem.2012.06.013.
[20] F. Zaccaria, C. Zuccaccia, R. Cipullo, A. Macchioni, Extraction of reliable molecular information from diffusion NMR spectroscopy: hydrodynamic volume or molecular mass? Chem. A Eur. J. 25 (2019) 9930–9937, https://doi.org/10.1002/chem.201900812.
[21] D.M. Duggan, D.N. Hendrickson, Electronic structure of various ferricenium systems as inferred from Raman, infrared, low-temperature electronic absorption, and electron paramagnetic resonance measurements, Inorg. Chem. 14 (1975) 955–970, https://doi.org/10.1021/ic50147a001.
[22] P.N. Bartlett, D. Cook, C.H. (Kees) de Groot, A.L. Hector, R. Huang, A. Jolleys, G. P. Kissling, W. Levason, S.J. Pearce, G. Reid, Non-aqueous electrodeposition of p-block metals and metalloids from halometallate salts, RSC Adv. 3 (2013) 15645–15654, https://doi.org/10.1039/c3ra40739j.
[23] D. Shoup, A. Szabo, Chronoamperometric current at finite disk electrodes, J. Electroanal. Chem. 140 (1982) 237–245, https://doi.org/10.1016/0022-0728(82)85171-1.
[24] M. Zistler, P. Wachter, P. Wasserscheid, D. Gerhard, A. Hinsch, R. Sastrawan, H. J. Gores, Comparison of electrochemical methods for triiodide diffusion coefficient measurements and observation of non-Stokesian diffusion behaviour in binary mixtures of two ionic liquids, Electrochim. Acta 52 (2006) 161–169, https://doi.org/10.1016/j.electacta.2006.04.050.
[25] D.L. Goldfarb, H.R. Corti, Steady-state voltammetric study of the reduction of decamethylferrocenium in dichloromethane at microelectrodes, J. Electroanal. Chem. 509 (2001) 155–162, https://doi.org/10.1016/S0022-0728(01)00530-7.
[26] Y. Marcus, The Properties of Solvents, Wiley, Chichester, 1998.
[27] L. De Lorenzi, M. Fermeglia, G. Torriano, Density and viscosity of 1-methoxy-2-propanol, 2-methyltetrahydrofuran, α,α,α-trifluorotoluene, and their binary mixtures with 1,1,1-trichloroethane at different temperatures, J. Chem. Eng. Data 41 (1996) 1121–1125, https://doi.org/10.1021/je9601220.
[28] O. Ivanciuc, T. Ivanciuc, P.A. Filip, D. Cabrol-Bass, Estimation of the liquid viscosity of organic compounds with a quantitative structure-property model, J. Chem. Inf. Comput. Sci. 39 (1999) 515–524, https://doi.org/10.1021/ci980117v.
[29] R.A. Robinson, R.H. Stokes, Electrolyte Solutions, 2nd ed., Butterworths, London, 1965 revised.
[30] D.M.P. Mingos, A.L. Rohl, Size and shape characteristics of inorganic molecules and ions and their relevance to molecular packing problems, J. Chem. Soc. Dalton Trans. (1991) 3419–3425, https://doi.org/10.1039/DT9910003419.
[31] G.Y. Ahlijah, M. Goldstein, Far-infrared and Raman spectra of tetrahalogeno-complexes of arsenic(III), antimony(III), and bismuth(III), J. Chem. Soc. A Inorg. Phys. Theor. 326 (1970), https://doi.org/10.1039/j19700000326.
[32] F.S.T. Khan, A.L. Waldbusser, M.C. Carrasco, H. Pourhadi, S. Hematian, Synthetic, spectroscopic, structural, and electrochemical investigations of ferricenium derivatives with weakly coordinating anions: ion pairing, substituent, and solvent effects, Dalton Trans. 50 (2021) 7433–7455, https://doi.org/10.1039/d1dt01192h.
[33] Y. Marcus, G. Hefter, Ion pairing, Chem. Rev. 106 (2006) 4585–4621, https://doi.org/10.1021/cr040087x.
[34] Y. Marcus, Ions in Solution and Their Solvation, Wiley, Hoboken, NJ, 2015.
[35] Y. Marcus, Are ionic stokes radii of any use? J. Solut. Chem. 41 (2012) 2082–2090, https://doi.org/10.1007/s10953-012-9922-4.
[36] W. Levason, G. Reid, J.A. McCleverty, T.J. Mayer, The coordination chemistry of arsenic, antimony, and bismuth. Comprehensive Coordination Chemistry II, Elsevier, Amsterdam, 2003, pp. 465–544, https://doi.org/10.1016/B0-08-043748-6/02023-5.
[37] R.G. Lin, G. Xu, G. Lu, M.S. Wang, P.X. Li, G.C. Guo, Photochromic hybrid containing *in situ* -generated benzyl viologen and novel trinuclear [Bi3Cl14]5-: improved photoresponsive behavior by the φ···φ interactions and size effect of inorganic oligomer, Inorg. Chem. 53 (2014) 5538–5545, https://doi.org/10.1021/ic5002144.
[38] C. Ji, Z. Sun, A. Zeb, S. Liu, J. Zhang, M. Hong, J. Luo, Bandgap narrowing of lead-free perovskite-type hybrids for visible-light-absorbing ferroelectric semiconductors, J. Phys. Chem. Lett. 8 (2017) 2012–2018, https://doi.org/10.1021/acs.jpclett.7b00673.
[39] P. Atkins, J. de Paula, Physical Chemistry, 10th ed., Oxford University Press, Oxford, 2014.